

Document downloaded from:

<http://hdl.handle.net/10251/201924>

This paper must be cited as:

Guntupalli, L.; Martínez Bauset, J.; Li, FY. (2018). Performance of Frame Transmissions and Event-triggered Sleeping in Duty-Cycled WSNs with Error-Prone Wireless Links. *Computer Networks*. 134:215-227. <https://doi.org/10.1016/j.comnet.2018.01.047>



The final publication is available at

<https://doi.org/10.1016/j.comnet.2018.01.047>

Copyright Elsevier

Additional Information

Performance of Frame Transmissions and Event-Triggered Sleeping in Duty-Cycled WSNs with Error-Prone Wireless Links

Lakshmikanth Guntupalli^a, Jorge Martinez-Bauset^b, Frank Y. Li^{a,*}

^a*Dept. of Information and Communication Technology, University of Agder (UiA), N-4898 Grimstad, Norway*

^b*Instituto ITACA, Universitat Politècnica de València (UPV), Camino de Vera s/n, 46022 València, Spain*

Abstract

Two types of packet transmission schemes are prevalent in duty-cycled wireless sensor networks, i.e., single packet transmission and aggregated packet transmission which integrates multiple packets in one frame. While most existing models are developed based on an error-free channel assumption, this paper evaluates the performance of both transmission schemes under error-prone channel conditions. We develop a four-dimensional discrete-time Markov chain model to investigate the impact of channel impairments on the performance of frame transmissions. Together with tracking the number of packets in the queue, number of retransmissions and number of active nodes, the fourth dimension of the model is able to capture the channel behavior at the frame-level. Based on the developed model, we analyze packet loss probability, packet delay, throughput, node energy consumption, and energy efficiency under various channel conditions. To further reduce energy consumption, we propose an event-triggered sleeping (ETS) energy mode for synchronous duty-cycling medium access control protocols. Numerical results reveal to which extent channel impairments may deteriorate the network performance, as well as the advantage of adopting aggregated packet transmission. The benefit brought by the ETS energy mode

*Corresponding author
Email address: frank.li@uia.no (Frank Y. Li)

is also demonstrated showing that the network lifetime is considerably extended, particularly in low traffic load scenarios.

Keywords: Duty-cycled WSNs, frame transmission, error-prone channels, event-triggered sleeping, discrete-time Markov chain, performance evaluation

1. Introduction

The integration of wireless sensor networks (WSNs) with the Internet of Things (IoT) [1] is an emerging trend towards a networked society. The IoT with sensor nodes offers a variety of applications from industrial automation, smart cities and smart grid, to environmental surveillance and protection. In many IoT applications, high energy efficiency and short packet delivery delay are essential requirements for the design of efficient medium access control (MAC) protocols in battery-powered WSNs [2]. Traditionally, duty-cycling (DC) has been a popular approach for energy conservation in WSNs. This mechanism allows us to organize the operation of a WSN into cycles. During each cycle, sensors wake up for packet transmission or reception and sleep for the rest of the cycle.

1.1. Motivation

For performance evaluation of frame transmission protocols in wireless networks, perfect channel condition is adopted in order to highlight the correctness of protocol operation. In reality, however, wireless channels are prone to errors. For instance, the channel conditions in environments where industrial WSNs are deployed are generally harsh and hostile [5]. Similar channel conditions are observed in smart grid applications as well [6]. Therefore, in order to assess the realistic behavior of a designed protocol, error-prone (EP) channel conditions need to be considered.

For frame transmissions in WSNs, failures happen primarily due to three reasons, i.e., medium access collision, buffer overflow, as well as poor channel conditions. Clearly, those frames which incurred transmission failures need to

25 be retransmitted and stay in the queue until they are delivered successfully,
or the retry limit is reached. Correspondingly longer packet delivery delay
and higher energy consumption would be expected in EP channel conditions.
Another characteristic of frame transmission over an EP link is that the failure
rate is frame length dependent. Typically, the success rate for transmitting
30 a short frame is higher than for a long frame [7]. **Failures based on the
channel impairments are frame length dependent. Large frame size
may be easily impacted by channel errors due to longer transmission
time. This will lead to an increase in the number of retransmissions.
Short packets consume less transmission time and have less possibility
35 of effected by the channel changes during transmissions, although
they contain more overhead messages than longer packets. Therefore,
frame length is essential for analyzing a protocol over a EP channel
in order to find out which is better either APT or SPT with EP
channel. This analysis could provide the insights to further determine
40 an optimized frame length to transmit for achieving a higher energy
efficiency.** Therefore, performance models that assess the impact of errors by
taking into account that the length of the transmitted frames might change from
cycle to cycle lead to more realistic results.

1.2. Contributions

45 In this paper, we investigate the performance of frame transmissions under
EP channel conditions. For this purpose, we model the evolution of the state of
the network over time by a four-dimensional (4D) discrete-time Markov chain
(DTMC). The impact of the channel state is represented by a frame-level error
model, that describes the occurrence of alternate bursts of cycles of random
50 length where frames are either transmitted successfully or failed. The channel
model considers also that a longer frame has a higher transmission failure prob-
ability compared with a shorter frame. Based on the proposed 4D model, we
develop expressions for packet delay, packet loss probability, throughput, node
energy consumption and energy efficiency for a WSN whose operation is based

55 on synchronous DC MAC protocols over EP links.

Furthermore, we observe that overhearing occurs often when employing synchronous DC protocols WSNs [8] and this problem becomes more severe in a network with multiple contending nodes. Considering that overhearing is typically caused by MAC protocol control packets, we propose an event-triggered sleeping (ETS) energy mode in order to improve the energy performance of frame transmissions. The main idea of the ETS energy mode is to allow nodes that do not have packets to send to sleep right after the synchronization phase, without participating in medium access contention. Then, inactive nodes can sleep longer, resulting in lower energy consumption. The ETS energy mode applies to synchronous DC protocols and suits ideally for WSN scenarios with a low traffic load. Correspondingly, the behavior of the ETS energy mode has been included in the developed 4D DTMC model.

In brief, the main contributions of this paper are summarized as follows.

- A novel 4D DTMC model for performance evaluation of frame transmissions in WSNs with error-prone links is developed. In addition to tracking the number of packets in a queue, the number of transmissions and the number of active nodes, the model has one dedicated dimension to represent channel conditions.
- Based on the developed 4D DTMC, closed-form expressions for performance parameters such as mean packet delay, throughput, packet loss probability, energy consumption, and energy efficiency are deduced. Although these calculations are tailored based on a specific DC MAC protocol S-MAC [9], the 4D model applies to other synchronous MAC protocols as well.
- An event-triggered sleeping energy mode for synchronous DC MAC protocols has been proposed, targeting at energy saving for frame transmissions at low traffic loads. Accordingly, its performance over error-prone links has been evaluated based on the developed 4D DTMC model.

- The accuracy of the developed 4D DTMC model has been validated using
85 discrete-event simulations.

The rest of this paper is organized as follows. After summarizing the related work in Section 2, we present the network scenario and protocol design in Section 3. The 4D DTMC model is developed in Section 4. Then, the expressions for performance metrics are derived in Sections 5 and 6 respectively.
90 In Section 7, we present the numerical results obtained by the proposed analytical model and discrete-event simulations. Finally, the paper is concluded in Section 8.

2. Related Work

In typical duty-cycled WSNs, single packet transmission (SPT) is adopted,
95 meaning that only one packet is transmitted per cycle once a node obtains medium access. On the contrary, when aggregated packet transmission (APT) is employed, a node might transmit multiple packets together (forming a *frame*) per cycle [3]. APT has the potential to increase energy efficiency and reduce packet delivery delay [4]. Consequently, APT appears as a promising technique
100 for *small data* transmission in many IoT applications. As SPT is a particular case of APT, where each frame contains only one packet, we refer to frames instead of packets as the transmission data units hereafter. In this section, we first summarize DTMC models developed for frame transmission under EF and EP channel conditions and then outline the frame-level channel error models.

105 2.1. DTMC Models for Frame Transmission with EF Links

In our earlier work [3], we proposed an analytical model to evaluate the performance of an APT scheme operating over a synchronous duty-cycled MAC protocol, S-MAC. The developed model therein was a three-dimensional (3D) DTMC, with each dimension representing the number of packets in the queue
110 of an arbitrarily selected node that we refer to as the reference node (RN), the number of retransmissions experienced by the frame at the head of the queue of

the RN, and the number of active nodes in the network (those with a non-empty queue). Unlike many other existing models for duty-cycled MAC protocols, the third dimension of the state vector of the proposed DTMC therein facilitates to track the evolution of the number of active nodes in the network over time. In this way, the dependency among nodes is traced.

However, the 3D DTMC model developed in our previous work [3] [10], and also those proposed by many other related studies [11] [13] were conceived under the assumption that the channel was error-free.

Exiting versus developed: Generally, the dimensions to consider in our DTMC modeling are the following

- (i) number of packets in the queue of the RN;
- (ii) number of nodes in the studied network or cluster;
- (iii) number of retransmissions allowed for each packet or frame;
- (iv) the channel is considered as error-free or not.

To clarify the difference between our models and the previous models, let i be the the number of packets found at the queue of the RN, k be the number of *active* nodes in the network and r be the number of retransmissions experienced by the packet at the head of the queue of the node. If only one parameter is modeled, we need only one dimension in a model and refer it to as one dimensional (1D) DTMC. Similarly, if a combination of two parameters is included, then the model is a 2D DTMC. In other words, a 3D DTMC models all the aforementioned three parameters when the channel is assumed to be error-free.

The distinction between the DTMC models developed for DC MAC protocols in the literature is illustrated in Fig. 2. A 1D DTMC studied in [11] considered only i . The previous 2D DTMCs in [12] and [13] modeled both i and r . As such, a novel 2D DTMC is defined by (i, k) in [3], and it is different from existing combinations

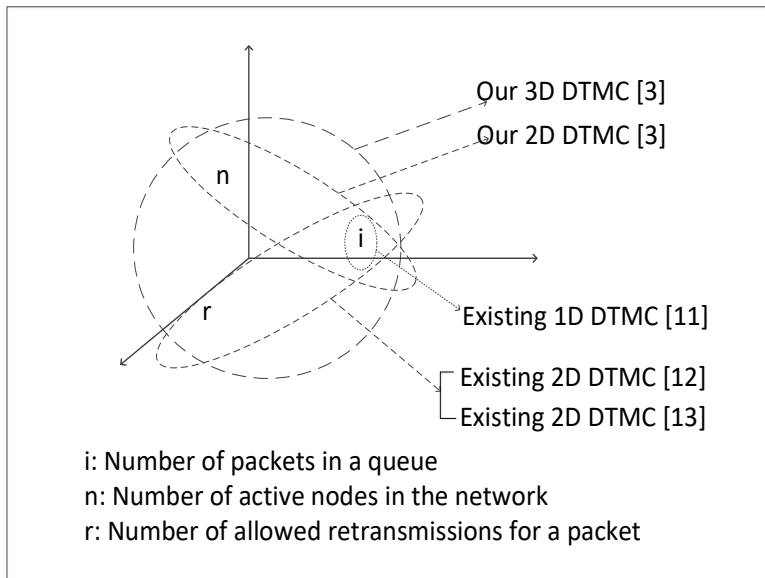


Figure 2: Illustration of the DTMC models for DC MAC protocols: existing versus ours.

in [12] and [13]. It is worth mentioning that 2D DTMC with the same dimensions are developed to evaluate APT, SPT and cooperative transmission in [8], [3] and [14] respectively. In addition, a 3D DTMC is developed by a triplet (i, k, r) to evaluate APT in [3]. Differently, in this paper, we have developed a 4D DTMC which contains channel condition as the fourth dimension. Furthermore, more detailed descriptions of the 4D DTMC and the closed-form expressions for performance parameters are also presented.

2.2. DTMC Models for Frame Transmission with EP Links

On other hand, there exist a number of models to analyze wireless links with errors. The effect of the frame length on channel errors in WSNs was studied in [7]. A similar study was performed for terrestrial, underwater and underground WSNs [21]. Likewise, the impact of retransmissions induced by the frame errors was investigated in [23] [22]. However, the authors therein did not take MAC protocols into account and their analysis focused only on PHY and link layer parameters. As such, [6] and [24] analyzed lifetime of WSNs under

harsh wireless links, however, only for TDMA based MAC protocols without
 160 considering MAC collisions. A few other models [25] [26] [27] evaluated the
 performance of MAC protocols in the presence of frame errors, but these models
 did not distinguish failures occurred due to transmission collisions and poor
 channel conditions. **Similarly, recent studies in [15] [16] and the
 analytical works in [17] [18] [19] evaluated contention based MAC
 165 protocols however those do not apply for duty-cycled MAC protocols.
 Although duty-cycled protocols were studied in [20], there channel
 access competition was not considered.**

In contrast, the model developed in this paper evaluates the impact of chan-
 nel conditions on WSN performance based on a carrier sense multiple access
 170 with collision avoidance (CSMA/CA) duty-cycled MAC protocol. It is worth
 mentioning that this model incorporates the dependence of frame errors under
 various channel conditions with the frame length.

2.3. Modeling of Frame-level Channel Errors

Among existing error models proposed to represent channel behavior, the
 175 *On/Off* model is a pragmatic and popular one [28] [30]. The *On/Off* model
 describes the holding times in the *On* (*loss*) and *Off* (*non-loss*) macro-states by
 a mixture of geometric distributions [28]. By *loss* we refer to operating cycles
 where a frame transmitted might fail due to channel errors. Whereas by *non-*
loss we refer to cycles during which successful transmissions occur, provided
 180 that the transmitted frames do not collide.

To capture the burstiness of channel behavior, a simple-yet-effective model
 was proposed in [31]. This model captures both first- and second-order statistics
 accurately and is considered as adequate to characterize wireless channels in
 realistic scenarios [28, 30]. The model exhibits a self-similar behavior over a
 185 configurable (finite) range of time-scales. One of its main advantages is its
 configuration simplicity, as it has only three parameters. One parameter allows
 to determine the range of time-scales where the process can be considered as
 self-similar. The other two allow to configure the rate of cycles with EP channel

conditions, referred to as EP cycle rate (ECR), and the average number of
190 consecutive cycles (burst) where the channel is in the EP state.

3. Network Scenario and Preliminaries

In this section, we first present the considered network scenario and then summarize the main features of S-MAC, which is a representative synchronous MAC protocol. The proposed ETS energy mode is explained afterwards.

195 3.1. Network Scenario

Consider a network, or a network cluster, consisting of N member nodes, where all nodes in the cluster can hear each other. The nodes are operated based on a synchronous DC MAC protocol and they have a homogeneous behavior. The frames are transmitted towards a common destination (a sink node) following a CSMA/CA contention-based mechanism with request to sent (RTS)/clear
200 to send (CTS)/DATA/ACK handshakes for channel access.

We select one of these cluster member nodes arbitrarily and refer to it as the reference node. The buffer of each node can store up to Q packets. Once a node wins access competition to the channel, it transmits a *frame* that aggregates
205 up to F packets. If $F = 1$, the transmission is performed based on SPT. For $F > 1$, the APT scheme is adopted. However, a transmitted frame may not be correctly received, due to either a collision or poor channel conditions. If the transmission is not successful, a node performs up to R retransmissions. The packets that compose a frame are deleted from the queue either when a frame
210 is successfully transmitted, or after R unsuccessful retransmissions.

3.2. A Synchronous DC MAC Protocol: S-MAC

Among existing synchronous MAC protocols in DC enabled WSNs, S-MAC is a representative one [9]. With S-MAC, nodes first agree to wake up at the same time periodically. At the wake-up instant, nodes exchange their next
215 schedule during a specific time period, referred to as a *sync* period, in order to wake up simultaneously after a *sleep* period. Schedules are exchanged by SYNC

packets. After the *sync* period, frame exchange is performed in the subsequent *data* period before going to sleep. The time elapsed between two consecutive wake-up instants is referred to as a *cycle*. Thus, one *cycle* consists of a *sync*, a *data* and a *sleep* period, as shown in Figure 1.

Another salient feature of S-MAC is that nodes keep awake for the whole duration of some cycles, in order to ensure the reception of SYNC packets. Such cycles are referred to as *awake* cycles, whereas *normal* cycles contain a *sleep* period.

Note that throughout this paper we use capital letters to represent the type of a packet, e.g., DATA, SYNC, and RTS, and lowercase letters to represent different parts of a cycle, i.e., *sync*, *data*, and *sleep*.

3.3. Event-Triggered Sleeping

In both *sync* and *data* periods, nodes follow the CSMA/CA mechanism for frame transmissions. In the conventional S-MAC operation nodes follow the control packet-triggered sleeping (CPTS) mode. When a node wins channel access it transmits a control packet, i.e., the RTS packet, informing the neighbor nodes about a subsequent frame transmission, as shown in Figure 1. All network nodes, regardless they are active or inactive, receive and decode this control packet to identify the destination address of the forthcoming frame. Only the destination node responds with a CTS packet and remains awake, while the rest of the nodes go to sleep. When the network operates in the CPTS mode, and particularly under low traffic loads, energy consumption is wasted in cycles in which no nodes are active. This phenomenon might happen in a noticeable fraction of cycles. In those cycles, all nodes remain awake until the end of the contention window waiting for the reception of an RTS packet that rarely or never happens.

In the studied scenario, however, nodes only transmit to the sink, and the sink does not transmit as it functions as a receiver only. The proposed ETS energy mode reduces energy consumption by letting inactive nodes go to sleep right at the beginning of the *data* period. In addition, active nodes that contend

for channel access in a cycle, save energy if they go right to sleep as soon as they detect channel activity before their backoff timers expire. In both situations, nodes following the ETS mode save energy by avoiding the reception and decoding the RTS packet.

3.4. Contention for Medium Access

For channel access in both CPTS and ETS, all *active* nodes generate a random backoff time from a uniformly distributed window $\{0, W - 1\}$ at the beginning of every *data* period. If the smallest backoff time is selected *by only one node*, then that node wins channel access and reserves the medium for a frame transmission in the subsequent *sleep* period. If a node selects a backoff time which is not the smallest one, it loses the competition and waits until the next *data* period to compete again. In case that the same smallest backoff time is selected by two or more nodes, then a collision occurs.

Consider $k + 1$ active nodes including the RN in a cycle. When the RN is contending with other k nodes, $0 \leq k \leq N - 1$, the probabilities that the RN transmits a packet successfully, $P_{s,k}$, or transmits a packet (successfully or with collision), $P_{sf,k}$, are given by

$$P_{s,k} = \sum_{i=0}^{W-1} \frac{1}{W} \left(\frac{W-1-i}{W} \right)^k, \quad (1)$$

$$P_{sf,k} = \sum_{i=0}^{W-1} \frac{1}{W} \left(\frac{W-i}{W} \right)^k. \quad (2)$$

Clearly, the probabilities that the RN transmits a packet with failure (collision), is given by $P_{f,k} = P_{sf,k} - P_{s,k} = 1/W$. The average length of the shortest backoff time in a cycle where a successful or failed transmission occurs is determined

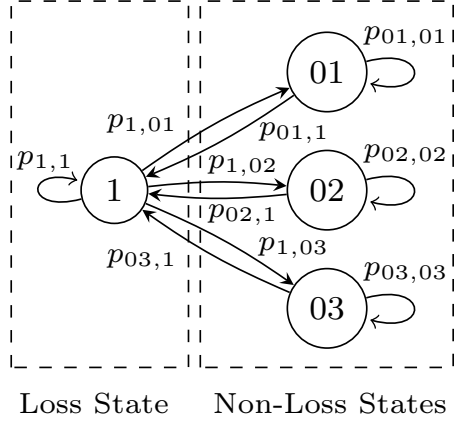


Figure 3: A frame-level error model for error-prone channels with one state in the *loss* macro-state and three states in the *non-loss* macro-state.

respectively by

$$BT_{s,k} = \frac{1}{P_{s,k}} \sum_{i=0}^{W-1} i \cdot \frac{1}{W} \left(\frac{W-1-i}{W} \right)^k, \quad (3)$$

$$BT_{f,k} = \sum_{i=0}^{W-1} i \cdot \left[\left(\frac{W-i}{W} \right)^k - \left(\frac{W-1-i}{W} \right)^k \right], \quad (4)$$

260 3.5. Channel Model for Frame-level Errors

The model developed in [31] has three parameters, H , a and b . H determines the range of time-scales where a process can be considered as self-similar. Once H is set, the ECR which indicates the rate of cycles with EP channel conditions is obtain by $\rho_E = (1 - 1/b)/(1 - 1/b^H)$. Furthermore, the average number
 265 of consecutive cycles (burst) where the channel is in the EP state is given by $E[B_E] = (\sum_{k=1}^{H-1} a^{-k})^{-1}$.

Its transition matrix is given by

$$\left[\begin{array}{c|cccc} 1 - \sum_{k=1}^{H-1} \alpha^k & \alpha^1 & \alpha^2 & \dots & \alpha^{H-1} \\ \hline \beta & 1 - \beta & & & \\ \beta^2 & & 1 - \beta^2 & & \\ \vdots & & & \ddots & \\ \beta^{H-1} & & & & 1 - \beta^{H-1} \end{array} \right]. \quad (5)$$

where $\alpha = 1/a$ and $\beta^m = (b/a)^m$.

For simplicity, we assume that $H = 4$, although larger values for H apply also
 270 to this model. Accordingly, the state and transition diagram of the frame-level
 error model is shown in Figure 3. The corresponding transition probabilities
 are given by $p_{1,1} = 1 - \sum_{k=1}^{H-1} 1/a^k$, $p_{1,0m} = 1/a^m$, $p_{0m,1} = (b/a)^m$, and
 $p_{0m,0m} = 1 - (b/a)^m$ respectively, where $m = 1, 2, \dots, H - 1$.

4. Discrete-time Markov Chain Model

275 A network state in the developed 4D DTMC model is represented by (i, k, r, e) ,
 where i is the number of packets in the queue of the RN and $i \leq Q$; k is the
 number of active nodes other than the RN in the network, $k \leq N - 1$; r is the
 number of retransmissions experienced by the frame at the head of the queue
 of the RN, $r \leq R$; and e represents a *loss* or *non-loss* channel state, as shown
 280 in Figure 3. When $e = 1$, a frame being transmitted without collision might
 not be received correctly due to channel errors. Whereas when $e = \{01, 02, 03\}$
 the transmitted frames will be received successfully, provided that they did not
 collide. For expression simplicity, we enumerate the e states as $\{1, 2, 3, 4\}$, where
 states $\{2, 3, 4\}$ correspond to $\{01, 02, 03\}$ in Figure 3.

Let \mathbf{P} be the transition matrix that defines the time evolution of the state

of the network. It has the following block structure

$$P = \left[\begin{array}{c|ccc} \mathbf{A}_0 & \mathbf{A}_1 & \mathbf{A}_2 & \mathbf{A}_3 \\ \hline \mathbf{B}_1 & \mathbf{B}_4 & \mathbf{0} & \mathbf{0} \\ \mathbf{B}_2 & \mathbf{0} & \mathbf{B}_5 & \mathbf{0} \\ \mathbf{B}_3 & \mathbf{0} & \mathbf{0} & \mathbf{B}_6 \end{array} \right]. \quad (6)$$

285 where $\mathbf{A}_0 = p_{1,1}\mathbf{P}_E$, and $\mathbf{A}_m = p_{1,0m}\mathbf{P}_E$. Similarly, $\mathbf{B}_m = p_{0m,1}\mathbf{P}_{NE}$, $\mathbf{B}_n = p_{0m,0m}\mathbf{P}_{NE}$, $m = 1, 2, 3$, $n = m + 3$. Note that matrices \mathbf{P}_{NE} and \mathbf{P}_E define the network behavior under the error-free and error-prone channel conditions respectively.

Transition matrix \mathbf{P}_E is shown in Table .3 of the Appendix. Observe that
 290 the EP channel behavior is characterized by S_i^e , which is the probability that a frame with a length of i packets is received with no channel errors, provided it did not collide. As an example, we configure it as $\{S_i^e\} = \{0.5, 0.4, 0.2, 0.1, 0.05\}$, for $i = 1, \dots, 5$. Clearly, the probability of successful reception of a longer frame ($S_5^e = 0.05$) is much lower than that for a shorter frame ($S_1^e = 0.5$).
 295 The configuration of S_i^e is scenario dependent, and it can be determined by measurements, historical information or other means. Note that by setting $S_i^e = 1, \forall i$, into \mathbf{P}_E , we obtain \mathbf{P}_{NE} .

4.1. Stationary Distribution

The steady-state probabilities $\boldsymbol{\pi} = \{\pi(i, k, r, e)\}$ can be obtained by solving the set of linear equations

$$\boldsymbol{\pi}P = \boldsymbol{\pi}, \boldsymbol{\pi}\mathbf{e} = \mathbf{1}, \quad (7)$$

where \mathbf{e} is a column vector of ones.

Denote by π_i the stationary probability of finding i packets at the queue of

the RN. It is given by,

$$\pi_i = \sum_{k=0}^K \sum_{r=0}^R \sum_{e=1}^4 \pi(i, k, r, e). \quad (8)$$

Let P_s be the average probability that the RN transmits a frame successfully in a random cycle, conditioned on it being active. It is given by,

$$\begin{aligned} P_s &= \frac{1}{G} \sum_{i=1}^Q \sum_{k=0}^K \sum_{r=0}^R \sum_{e=2}^4 \pi(i, k, r, e) \cdot P_{s,k} \\ &+ \frac{1}{G} \sum_{i=1}^Q \sum_{k=0}^K \sum_{r=0}^R \pi(i, k, r, 1) \cdot P_{s,k} S_\alpha^e, \end{aligned} \quad (9)$$

300 where $G = \sum_{i=1}^Q \sum_{k=0}^K \sum_{r=0}^R \sum_{e=1}^4 \pi(i, k, r, e)$ is the fraction of cycles in which the RN is active, $P_{s,k}$ is the probability that the RN transmits without collision when contending with the other k active nodes, and S_α^e is the probability that the transmission of a frame of length $\alpha = \min\{i, F\}$ is received without being in the loss state.

Let S^e be the fraction of cycles in the *loss* state ($e = 1$) where frame transmissions occur with no channel error, conditioned on the RN being active. Then,

$$S^e = \frac{1}{G^e} \sum_{i=1}^Q \sum_{k=0}^K \sum_{r=0}^R \pi(i, k, r, 1) \cdot S_\alpha^e, \quad (10)$$

305 where $G^e = \sum_{i=1}^Q \sum_{k=0}^K \sum_{r=0}^R \pi(i, k, r, 1)$.

Let P_e be the probability that the queue of an active node becomes empty after a successful transmission. Then,

$$P_e = \frac{P_s A_0 \sum_{i=1}^F \pi_i}{[P_s (1 - \pi_0)]}, \quad (11)$$

where A_0 is the probability that no packet arrived during the considered cycle.

Note that the transition probabilities in \mathbf{P} are given as a function of P_e and S^e . Then, the steady-state probabilities $\boldsymbol{\pi}$ are obtained as the solution of a

fixed-point equation.

310 5. Performance Expressions based on 4D DTMC

Once the stationary distribution $\boldsymbol{\pi}$ is obtained, we can derive expressions for the average packet delay, node and network throughput, packet loss probability, node energy consumption, and energy efficiency. It is worth mentioning that the expressions obtained in this section apply generally to any MAC protocols, as
315 long as they are operated in a synchronous duty-cycled manner. For additional details regarding the notations adopted, please refer to Table .3 in the Appendix.

5.1. Queuing Delay

Let us denote by D the average queuing delay of a packet, from its arrival until it is successfully delivered, i.e., it is transmitted neither with collision nor channel error. Then, by Little's law, D (in cycles) is equal to the average number of packets in the queue, N_{av} , divided by the average number of packets accepted by the node (stored in the queue) per cycle, γ_a . Then,

$$D = N_{av}/\gamma_a = \sum_{i=0}^Q i\pi_i/\gamma_a. \quad (12)$$

Note that γ_a can also be determined as the mean number of packets removed from the buffer of the RN per cycle. That is, the sum of the packets transmitted successfully plus those packets discarded because they exceeded the maximum

number of retransmissions. Then,

$$\begin{aligned}
\gamma_a &= \sum_{i=1}^Q \sum_{k=0}^K \sum_{r=0}^R \sum_{e=2}^4 \alpha \pi(i, k, r, e) \cdot P_{s,k} \\
&+ \sum_{i=1}^Q \sum_{k=0}^K \sum_{r=0}^R \alpha \pi(i, k, r, 1) \cdot P_{s,k} S_\alpha^e \\
&+ \sum_{i=1}^Q \sum_{k=0}^K \sum_{e=1}^4 \alpha \pi(i, k, R, e) \cdot P_{f,k} \\
&+ \sum_{i=1}^Q \sum_{k=0}^K \alpha \pi(i, k, R, 1) \cdot P_{s,k} (1 - S_\alpha^e) .
\end{aligned} \tag{13}$$

Recall that $\alpha = \min(i, F)$ is the number of packets aggregated in a frame, $1 \leq i \leq Q$, $P_{f,k}$ and $P_{s,k}$ are the probabilities of transmission with and without collision in a cycle where the RN contends with other k nodes, and S_α^e is the probability that a frame of length α is received with no errors.

5.2. Throughput

The throughput that a node achieves, denoted by η , is defined as the average number of packets it *successfully* delivers per cycle. Then,

$$\begin{aligned}
\eta &= \sum_{i=1}^Q \sum_{k=0}^K \sum_{r=0}^R \sum_{e=2}^4 \alpha \cdot \pi(i, k, r, e) \cdot P_{s,k} \\
&+ \sum_{i=1}^Q \sum_{k=0}^K \sum_{r=0}^R \alpha \cdot \pi(i, k, r, 1) \cdot P_{s,k} S_\alpha^e .
\end{aligned} \tag{14}$$

Given that there are N nodes in the studied network cluster, the total network throughput becomes

$$Th = N \cdot \eta . \tag{15}$$

5.3. Packet Loss Probability

Retransmissions occur due to frame collisions, or failed reception of frames due to channel errors. Moreover, a frame also gets lost (discarded from the

buffer) after R consecutive unsuccessful retransmissions. Denote by P_L^c the channel packet loss probability, i.e., the fraction of accepted packets that are lost due to collisions or channel errors. It is given by,

$$P_L^c = \frac{1}{\gamma_a} \sum_{i=1}^Q \sum_{k=0}^K \sum_{e=1}^4 \alpha \cdot \pi(i, k, R, e) \cdot P_{f,k} \quad (16)$$

$$+ \frac{1}{\gamma_a} \sum_{i=1}^Q \sum_{k=0}^K \alpha \cdot \pi(i, k, R, 1) \cdot P_{s,k} (1 - S_\alpha^e),$$

where γ_a is the average number of packets accepted into the queue of the RN per cycle, $P_{f,k}$ is the probability that a frame transmitted by the RN collides when contending with the other $k \geq 1$ nodes, and $P_{sf,k}$ is the probability that the RN transmits a frame (with or without collision).

Note that losses can also occur due to buffer overflow. To calculate the total packet loss probability, P_L , overflow losses must be added to P_L^c . Given a packet arrival rate λ and a cycle length T , the mean number of packets lost per cycle (packet loss rate) is $\lambda T - [(1 - P_L^c) \gamma_a]$. Then,

$$P_L = 1 - \frac{(1 - P_L^c) \gamma_a}{\lambda T}. \quad (17)$$

6. MAC Specific Energy Performance Analysis

Different from the above parameters, the expressions derived below for the calculation of the energy consumption are protocol specific. In this section, we adopt S-MAC and derive expressions for node energy consumption and energy efficiency when the network operates in the CPTS and ETS energy modes.

6.1. Energy Consumption based on the CPTS Mode

We calculate first the average energy consumption per cycle in the three periods (*sync*, *data* and *sleep*) and then obtain the energy efficiency.

6.1.1. Energy consumption in the sync period

Denote by T_{sync} the duration of a *sync* period. It is obtained as $T_{sync} = (W - 1) + t_{SYNC}$, as more than one node will rarely transmit simultaneously a SYNC packet. Assume that the RN *broadcasts* one *SYNC* packet every N_{sc} cycles and it listens to the medium for *SYNC* packets in the remaining $N_{sc} - 1$ cycles. Accordingly, the average energy consumed by the RN in the *sync* period is given by,

$$E_{sc} = [t_{SYNC}P_{tx} + (T_{sync} - t_{SYNC})P_{rx}]/N_{sc} + (N_{sc} - 1)T_{sync}P_{rx}/N_{sc}, \quad (18)$$

where P_{tx} and P_{rx} are the transmission and reception power levels respectively. Note that the RN consumes energy for carrier sensing as well when transmitting the *SYNC* packets, and this energy consumption is already included in the
340 second part of the first term in (18).

6.1.2. Energy consumption in the data period

The average energy consumed by a node in the *data* period is given by,

$$E_d^* = \sum_{k=0}^N E_{d,k} \cdot \pi'_{ne,k} + \tilde{E}_{d,k} \cdot \pi'_{e,k}, \quad (19)$$

where $E_{d,k+1}$ and $\tilde{E}_{d,k+1}$ are the average energy consumed by the RN when it contends with the other $k \geq 1$ nodes during the *data* period of cycles in the *non-loss* and *loss* macro-states, respectively; and $\pi'_{e,k}$ and $\pi'_{ne,k}$ are the stationary probability of finding k active nodes in the network during cycles in the *loss* and *non-loss* macro-states, respectively. They are obtained as $\pi'_{e,k} = \sum_{i=1}^Q \sum_{r=0}^R \pi(i, k - 1, r, 1) + \pi(0, k, 0, 1)$, $\pi'_{ne,k} = \sum_{i=1}^Q \sum_{r=0}^R \sum_{e=2}^4 \pi(i, k - 1, r, e) + \sum_{e=2}^4 \pi(0, k, 0, e)$, for $1 \leq k \leq N - 1$. For $k = 0$ and $k = N$, we have $\pi'_{e,0} = \pi(0, 0, 0, 1)$, $\pi'_{ne,0} = \sum_{e=2}^4 \pi(0, 0, 0, e)$, $\pi'_{e,N} = \sum_{i=1}^Q \sum_{r=0}^R \pi(i, N - 1, r, 1)$,
345 $\pi'_{ne,N} = \sum_{i=1}^Q \sum_{r=0}^R \sum_{e=2}^4 \pi(i, N - 1, r, e)$.
350

Denote by $f_{ne,k}$ and $f_{e,k}$ the mean frame length of those frames transmitted

in *non-loss* and *non-loss* cycles where the RN contends with the other k ($0 \leq k < N$) nodes. We have

$$f_{ne,k} = \frac{1}{G_{ne,k}} \sum_{i=1}^Q \sum_{r=0}^R \sum_{e=2}^4 \alpha \cdot \pi(i, k, r, e), \quad (20)$$

$$f_{e,k} = \frac{1}{G_{e,k}} \sum_{i=1}^Q \sum_{r=0}^R \alpha \cdot \pi(i, k, r, 1), \quad (21)$$

where $G_{ne,k} = \sum_{i=1}^Q \sum_{r=0}^R \sum_{e=2}^4 \pi(i, k, r, e)$, and $G_{e,k} = \sum_{i=1}^Q \sum_{r=0}^R \pi(i, k, r, 1)$.

Let $S_{e,k}$ denote the mean rate of frames received with no channel error in the *loss* cycles when the RN contends with other k ($0 \leq k < N$) nodes. We have,

$$S_{e,k} = \frac{1}{G_{e,k}} \sum_{i=1}^Q \sum_{r=0}^R S_{\alpha}^e \cdot \pi(i, k, r, 1). \quad (22)$$

Conditioned on finding $k+1$ nodes active in a cycle, $q_{1,k} = (k+1)/N$ is the probability that the RN is active, $q_{2,k} = kq_{1,k} + (k+1)(1 - q_{1,k})$ is the average number of active nodes other than the RN, and $q_{3,k} = 1 - q_{2,k}P_{s,k} - q_{1,k}P_{sf,k}$ is the probability that nodes other than the RN transmit a frame with failure (collision). Then, for the *data* period in *non-loss* cycles, we obtain,

$$\begin{aligned} E_{d,k+1} &= q_{1,k} [P_{s,k} E_{s,k}^{tx} + P_{f,k} E_{f,k}^{tx}] + E_{oh,k}, \\ E_{s,k}^{tx} &= (t_{RTS} + f_{ne,k} \cdot t_{DATA}) P_{tx} \\ &\quad + (BT_{s,k} + t_{CTS} + t_{ACK} + 4D_p) P_{rx}, \\ E_{f,k}^{tx} &= t_{RTS} P_{tx} + (BT_{f,k} + 2D_p) P_{rx}, \\ E_{oh,k} &= q_{2,k} P_{s,k} [t_{RTS} P_{rx} + (BT_{s,k} + D_p) \cdot P_{rx}] \\ &\quad + q_{3,k} \cdot [t_{RTS} P_{rx} + (BT_{f,k} + D_p) \cdot P_{rx}], \end{aligned} \quad (23)$$

where t_{RTS} , t_{DATA} , t_{CTS} and t_{ACK} , are the corresponding packet transmission times, D_p is the one-way propagation delay, $E_{s,k}^{tx}$ is the average energy consumed by the RN to transmit a frame successfully, $E_{f,k}^{tx}$ is the average energy consumed

355 by the RN to transmit a frame with collision, and $E_{oh,k}$ is the average energy
 consumed by the RN due to overhearing frames successfully transmitted by
 other nodes and frames transmitted by other nodes that collide. Recall that
 $BT_{s,k}$ and $BT_{f,k}$ are the RN average backoff window lengths in cycles when the
 RN contends with other k nodes and the transmission occurs without and with
 360 collision, respectively.

For the data period in *loss* cycles, we have

$$\begin{aligned}
 \tilde{E}_{d,k+1} &= q_{1,k} P_{s,k} \left[S_{e,k} \tilde{E}_{s,k}^{tx} + (1 - S_{e,k}) \tilde{E}_{f,k}^{tx} \right] \\
 &\quad + q_{1,k} P_{f,k} E_{f,k}^{tx} + E_{oh,k}, \\
 \tilde{E}_{s,k}^{tx} &= (t_{RTS} + f_{e,k} \cdot t_{DATA}) P_{tx} \\
 &\quad + (BT_{s,k} + t_{CTS} + t_{ACK} + 4D_p) P_{rx}, \\
 \tilde{E}_{f,k}^{tx} &= \tilde{E}_{s,k}^{tx} - t_{ACK} P_{rx}.
 \end{aligned} \tag{24}$$

When the RN transmits a frame without collision but it is received with channel
 error, then the energy consumed by the RN is almost the same as when it
 arrives with no channel error, except that the ACK will not be received. When
 the frame transmitted by the RN collides, or when the RN overhears frames
 365 transmitted by other nodes, it has the same behavior as in *non-loss* cycles.

Note that $P_{s,0} = 1$, $P_{f,0} = 0$, $BT_{s,0} = (W - 1)/2$, $E_{d,1} = q_{1,0} E_{s,0}^{tx}$, $\tilde{E}_{d,1} =$
 $q_{1,0} \left[S_{e,0} \tilde{E}_{s,0}^{tx} + (1 - S_{e,0}) \tilde{E}_{f,0}^{tx} \right]$, and $E_{d,0} = \tilde{E}_{d,0} = (W + t_{RTS} + D_p) \cdot P_{rx}$.

6.1.3. Energy consumption in the sleep period

As explained in Section 3.2, nodes in S-MAC need to keep *awake* during the
 370 *sleep* period of some cycles in order to avoid missing synchronization messages.
 As mentioned earlier, such cycles are referred as *awake* cycles, whereas the cycles
 with nodes being asleep during *sleep* are referred as *normal* cycles. The average
 energy consumed during the *sleep* period of a cycle when the RN is *awake* is
 determined by

$$E_{aw}^* = \sum_{k=0}^N E_{aw,k} \cdot \pi'_{ne,k} + \tilde{E}_{aw,k} \cdot \pi'_{e,k}, \quad (25)$$

375 where $E_{aw,k+1}$ and $\tilde{E}_{aw,k+1}$ are the average energy consumed by the RN in
 cycles contending with other $k \geq 1$ active nodes, during the *sleep* period of
 380 *awake* cycles in the *non-loss* and *loss* macro-states respectively.

To determine the energy consumed during *awake* cycles, we consider when
 the RN is active (with probability $q_{1,k}$) and when it is not active. When it is
 380 active and it transmits a frame successfully in the *non-loss* cycles, it will remain
 awake after the end of the transmission. If the transmission fails, it will remain
 awake after the transmission of the RTS.

Regardless of the RN being active or inactive, when overhearing a successful
 transmission, it will sleep while the ongoing transmissions is performed. It will
 wake up when the transmission finishes and remain awake until the end of the
 cycle. Assume that the RN is able to infer the length of the frame transmission
 after decoding the RTS packet. When overhearing a transmission with collision,
 however, it will remain awake for the whole *data* (and *sleep*) period. Then we
 have,

$$\begin{aligned} E_{aw,k+1} &= q_{1,k} [P_{s,k} E_{s,k}^{aw} + P_{f,k} E_{f,k}^{aw} + k P_{s,k} E_{os,k}^{aw} \\ &\quad + (1 - k P_{s,k} - P_{sf,k}) E_{of,k}^{aw}] + (1 - q_{1,k}) \\ &\quad [(k+1) P_{s,k} E_{os,k}^{aw} + (1 - (k+1) P_{s,k}) E_{of,k}^{aw}] \\ E_{s,k}^{aw} &= (T - T_{sync} - B T_{s,k} - t_{RTS} - t_{CTS} \\ &\quad - f_{ne,k} \cdot t_{DATA} - t_{ACK} - 4D_p) P_{rx}, \\ E_{f,k}^{aw} &= (T - T_{sync} - B T_{f,k} - t_{RTS} - 2D_p) P_{rx}, \\ E_{os,k}^{aw} &= E_{s,k}^{aw} + (B T_{s,k} + t_{RTS} + D_p) P_{rx}, \\ E_{of,k}^{aw} &= (T - T_{sync}) P_{rx}. \end{aligned} \quad (26)$$

When being active in the *loss* cycles, if the RN transmits a frame with

neither collision nor channel error, it will remain awake after the end of the transmission. When it transmits a frame without collision but with channel error it will remain awake after realizing that the ACK will not be received until the end of the cycle. If the transmission of the RN fails and during overhearing, the RN behaves almost as in the *non-loss* cycles.

$$\begin{aligned}
\tilde{E}_{aw,k+1} &= q_{1,k} \left[P_{s,k} \tilde{E}_{d,k}^{aw} + P_{f,k} E_{f,k}^{aw} + k P_{s,k} \tilde{E}_{os,k}^{aw} \right. \\
&\quad \left. + (1 - k P_{s,k} - P_{sf,k}) E_{of,k}^{aw} \right] + (1 - q_{1,k}) \\
&\quad \left[(k+1) P_{s,k} \tilde{E}_{os,k}^{aw} + (1 - (k+1) P_{s,k}) E_{of,k}^{aw} \right] \\
\tilde{E}_{d,k}^{aw} &= S_{e,k} \tilde{E}_{s,k}^{aw} + (1 - S_{e,k}) \tilde{E}_{f,k}^{aw}, \\
\tilde{E}_{s,k}^{aw} &= (T - T_{sync} - B T_{s,k} - t_{RTS} - t_{CTS} \\
&\quad - f_{e,k} \cdot t_{DATA} - t_{ACK} - 4D_p) P_{rx}, \\
\tilde{E}_{f,k}^{aw} &= \tilde{E}_{s,k}^{aw} + t_{ACK} P_{rx}, \\
\tilde{E}_{os,k}^{aw} &= \tilde{E}_{s,k}^{aw} + (B T_{s,k} + t_{RTS} + D_p) P_{rx}. \tag{27}
\end{aligned}$$

Note that $E_{aw,1} = q_{1,0} E_{s,0}^{aw} + (1 - q_{1,0}) E_{os,0}^{aw}$, $\tilde{E}_{aw,1} = q_{1,0} \tilde{E}_{d,0}^{aw} + (1 - q_{1,0}) \tilde{E}_{os,0}^{aw}$, and $E_{aw,0} = \tilde{E}_{aw,0} = (T - T_{sync}) P_{rx}$.

Similarly, the average energy consumed during the *sleep* period of a cycle in *normal* cycles is given by

$$E_{nr}^* = \sum_{k=0}^N E_{nr,k} \cdot \pi'_{ne,k} + \tilde{E}_{nr,k} \cdot \pi'_{e,k}, \tag{28}$$

385 where $E_{nr,k+1}$ and $\tilde{E}_{nr,k+1}$ are the average energy consumed by the RN during the *sleep* period of a *normal* cycle under the *non-loss* and *loss* macro-state respectively, conditioned on cycles in which the RN and other $k \geq 1$ nodes are active. Terms $E_{nr,k+1}$ and $\tilde{E}_{nr,k+1}$ have the same expressions as $E_{aw,k+1}$ and $\tilde{E}_{aw,k+1}$, respectively, but the reception power P_{rx} needs to be replaced by the
390 sleep power P_{sl} .

Consider that the RN follows *awake* cycles during N_{sc} consecutive cycles,

whereas it follows *normal* cycles during the other $(N_{aw} - 1) \cdot N_{sc}$ consecutive cycles. Then, the average energy consumption during the *sleep* period of a cycle is obtained by

$$E_{sl}^* = \frac{E_{nr}^* \cdot N_{sc} \cdot (N_{aw} - 1) + E_{aw}^* \cdot N_{sc}}{N_{sc} \cdot N_{aw}}. \quad (29)$$

Therefore, the total average energy consumed by the RN in a cycle is obtained by

$$E^* = E_{sc} + E_d^* + E_{sl}^*. \quad (30)$$

The lifetime of the RN, i.e., the number of consecutive cycles the RN can operate with an initial energy $E_{initial}$ is determined by

$$LT = \frac{E_{initial}}{E} \text{ cycles}. \quad (31)$$

Lastly, the energy efficiency, ξ , expressed as the number of bytes successfully transmitted per energy unit consumed in a cycle, is given by

$$\xi = \eta \cdot S / E^*, \quad (32)$$

where S denotes the *frame* size in bytes.

6.2. Energy Consumption based on the ETS energy mode

Observe that when deploying the ETS energy mode, the RN sleeps during the *data* period when it is inactive. Also, it sleeps when it loses channel access contention when it is active. Note that the expressions for the energy consumption in the *sleep* period of *awake* cycles remain unchanged as we assume that the RN infers the length of the frame after decoding the RTS packet.

The expressions for $E_{d,k+1}$, $\tilde{E}_{d,k+1}$, $E_{nr,k+1}$, and $\tilde{E}_{nr,k+1}$ are redefined as,

$$\begin{aligned}
E_{d,k+1} &= q_{1,k} [P_{s,k} E_{s,k}^{tx} + P_{f,k} E_{f,k}^{tx} + E_{oh,k}] , \\
\tilde{E}_{d,k+1} &= q_{1,k} P_{s,k} [S_{e,k} \tilde{E}_{s,k}^{tx} + (1 - S_{e,k}) \tilde{E}_{f,k}^{tx}] \\
&\quad + q_{1,k} [P_{f,k} E_{f,k}^{tx} + E_{oh,k}] , \\
E_{oh,k} &= [k P_{s,k} (BT_{s,k} + D_p) \\
&\quad + (1 - k P_{s,k} - P_{sf,k}) (BT_{f,k} + D_p)] P_{rx} ,
\end{aligned} \tag{33}$$

$$\begin{aligned}
E_{nr,k+1} &= q_{1,k} [P_{s,k} E_{s,k}^{nr} + P_{f,k} E_{f,k}^{nr} + k P_{s,k} E_{os,k}^{nr} \\
&\quad + (1 - k P_{s,k} - P_{sf,k}) E_{of,k}^{nr}] + (1 - q_{1,k}) E_{ia}^{nr} , \\
E_{s,k}^{nr} &= (T - T_{sync} - BT_{s,k} - t_{RTS} - t_{CTS} \\
&\quad - f_{ne,k} \cdot t_{DATA} - t_{ACK} - 4D_p) P_{sl} , \\
E_{f,k}^{nr} &= (T - T_{sync} - BT_{f,k} - t_{RTS} - 2D_p) P_{sl} , \\
E_{os,k}^{nr} &= (T - T_{sync}) P_{sl} + (BT_{s,k} + D_p) (P_{rx} - P_{sl}) , \\
E_{of,k}^{nr} &= (T - T_{sync}) P_{sl} + (BT_{f,k} + D_p) (P_{rx} - P_{sl}) , \\
E_{ia}^{nr} &= (T - T_{sync}) P_{sl} .
\end{aligned} \tag{34}$$

$$\begin{aligned}
\tilde{E}_{nr,k+1} &= q_{1,k} [P_{s,k} \tilde{E}_{d,k}^{nr} + P_{f,k} E_{f,k}^{nr} + k P_{s,k} E_{os,k}^{nr} \\
&\quad + (1 - k P_{s,k} - P_{sf,k}) E_{of,k}^{nr}] + (1 - q_{1,k}) E_{ia}^{nr} , \\
\tilde{E}_{d,k}^{nr} &= S_{e,k} \tilde{E}_{s,k}^{nr} + (1 - S_{e,k}) \tilde{E}_{f,k}^{nr} , \\
\tilde{E}_{s,k}^{nr} &= (T - T_{sync} - BT_{s,k} - t_{RTS} - t_{CTS} \\
&\quad - f_{e,k} \cdot t_{DATA} - t_{ACK} - 4D_p) P_{sl} , \\
\tilde{E}_{f,k}^{nr} &= \tilde{E}_{s,k}^{nr} - t_{ACK} P_{sl} .
\end{aligned} \tag{35}$$

When the number of active nodes is zero, the energy consumption in the
400 network is also zero, i.e., $E_{d,0} = \tilde{E}_{d,0} = 0$.

7. Numerical Results

In this section we evaluate the performance of a WSN, where the operation of the nodes is based on a synchronous DC MAC protocol. The numerical results below are obtained based on a network with the following reference configuration. A network with $N = 15$ nodes, each with a queue capacity of $Q = 10$ packets, an identical *DATA* packet size of $S = 50$ bytes, the maximum number of retransmissions allowed as $R = 10$, and the packet arrival rate $\lambda \in [0, 2.5]$ packets/s. The configuration of the *awake* and *normal* cycles is defined as $N_{sc} = 10$, and $N_{aw} = 40$. For the APT scheme, the maximum number of packets per frame is $F \in \{1, 2, 5\}$. The transmission, reception and sleep power levels are: $P_{tx} = 52$ mW, $P_{rx} = 59$ mW, and $P_{sl} = 3$ μ W, respectively. To determine the lifetime of a node, we assume that it is charged with an initial energy $E_{initial} = 1$ J. The time parameters are summarized in Table 1.

Table 1: Time Parameters (unit: millisecond)

Cycle duration (T)	60	Propagation delay (D_p)	0.001
t_{RTS} , t_{CTS} and t_{ACK}	0.18	t_{SYNC}	0.18
t_{DATA}	1.716	Contention Window (W)	128

Given that $H = 4$, we obtain $b = 0.4418$ to achieve a rate of cycles in which error-prone channel conditions occur, i.e., ECR, of $\rho_E = 5\%$. Furthermore, $a = 2$ in order to obtain a mean frame-error burst length of $E[B_E] = 1.143$. These values lead to a realistic channel characterization according to field measurements [29]. Three channel conditions are defined, as error-free, lightly error-prone (LEP) and heavily error-prone (HEP). Under the HEP channel conditions the successful frame transmission probabilities are configured as $\{S_i^e\} = \{0.05, 0.02, 0.01, 0.005, 0.001\}$, where $i = 1..5$ indicate the frame lengths. Under the LEP channel conditions, they are set to $\{S_i^e\} = \{0.5, 0.4, 0.2, 0.1, 0.05\}$, where $i = 1..5$. Likewise, in the EF channel conditions $S_i^e = 1, \forall i$. Note that these probabilities indicate the successful delivery of frames to the sink, provided that no collision happened during frame transmission.

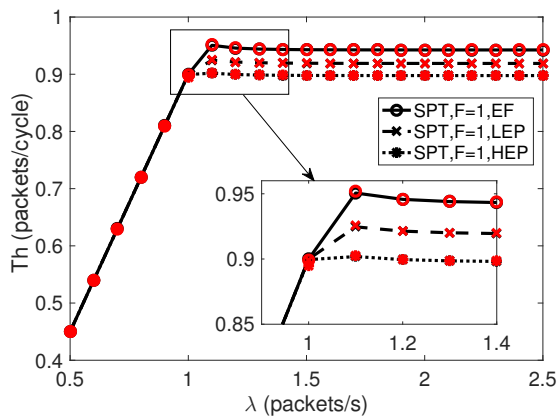


Figure 4: Throughput of SPT ($F = 1$) for different packet arrival rates under different channel conditions.

7.1. 4D DTMC Model Validation

We developed a custom-built discrete-event simulator where packets arrive to nodes stochastically and they might be queued at the node or get lost (overflow). In this network, nodes contend for channel access (if being active) in every cycle according to the adopted MAC protocol. When they gain channel access, they transmit frames over a channel under both EF and EP conditions. The simulations performed are completely independent of the expressions derived from the DTMC model. The simulation results presented below are averaged over $5 \cdot 10^6$ cycles. The confidence intervals are so small that, for clarity, they have not been displayed in the figures.

To assess the accuracy of the developed 4D DTMC model, we plot the analytical results together with the simulation results in all figures. The analytical results are produced from the expressions derived in Sections 5 and 6. The accuracy of the proposed models is demonstrated with all results as a relative error is lower than 1%. Note that the denominator of the relative error calculation, $|x - y| / y$, is y , indicating that the value obtained by simulation is considered to be more accurate and it is treated as the baseline value for this calculation. The results plotted in this section demonstrate that excellent

445 **precision of the analytical model has been achieved when determining performance parameters.** In all figures, the curves in black represent the analytical results, while simulation results are represented by only red markers.

As an example, Figure 4 shows the evolution of the total network throughput obtained by (15) for SPT with various packet arrival rates under different channel conditions. Clearly, both analytical and simulation results match precisely,
450 confirming that the developed analytical model is sufficiently accurate.

7.2. Performance of SPT in the CPTS Mode

Figure 4 illustrates the total throughput when the SPT scheme is employed under the EF, LEP and HEP channel conditions. As expected, the higher the error rate, the lower the throughput. For example, the throughput obtained
455 under the HEP and LEP channel condition is approximately 5% and 2.5% lower, respectively, than the one achieved in the EF channel condition. In addition, the network saturates earlier under a HEP channel ($\lambda = 1.0$ packet/s) than under an EF (1.1 packet/s) channel. This is because more packets wait in the
460 queue for retransmission under a HEP channel and therefore more nodes are active per cycle on average.

This effect is more vividly evident in the delay curves shown in Figure 5, where the saturation point is clearly marked by the sharp delay increase around $\lambda = 1.0$ packet/s. Below the saturation load, there is no or little access contention for channel access. Then, packets will be delivered immediately upon
465 arrival. Even in the case of packets being delivered with error due to channel impairment, packets are retransmitted almost immediately. As traffic load increases, more cycles are needed in order to deliver a packet successfully.

Figure 6 shows the evolution of the total packet loss probability with the load under three channel conditions. Clearly, losses start to increase noticeably after the saturation point, and the loss probability becomes higher with a poorer channel condition. As more packets need to be retransmitted due to poor channel conditions, more packets are stored in the queue on average, and the probability of a packet being lost due to overflow upon arrival increases.

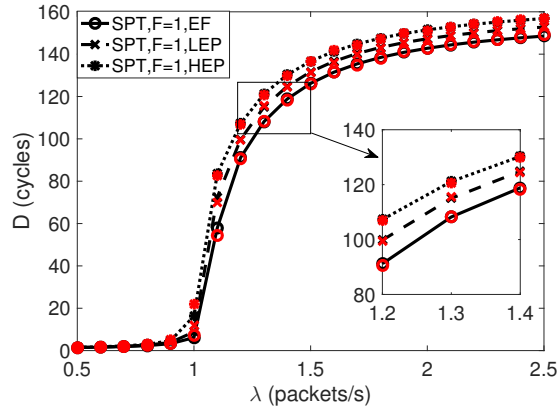


Figure 5: Delay of SPT ($F = 1$) for different packet arrival rates.

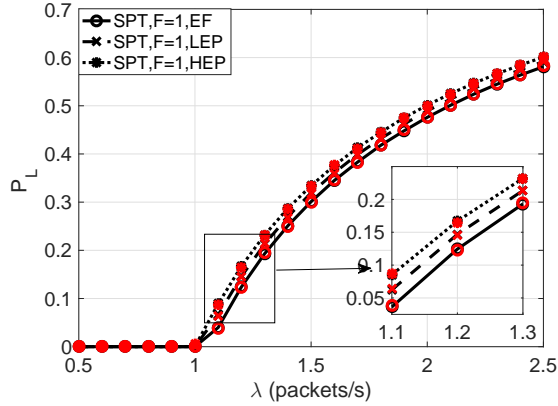


Figure 6: Packet loss of SPT ($F = 1$) for different packet arrival rates.

475 Figure 7 depicts the average energy consumed per cycle by a node deploying
SPT under different channel conditions. Clearly, two distinctive operating re-
gions can be observed: unsaturated and saturated. In the unsaturated region,
the packet arrival rate λ is low and there are many cycles with no active nodes
contending for channel access. When the network operates in the CPTS energy
480 mode, all network nodes waste energy in these cycles due to idle listening as
they wait for an RTS packet that will not arrive. As traffic load increases before
the saturation point, the energy consumption decreases due to less idle listening.
When the network is saturated, the consumed energy level stabilizes, as most
of the nodes are active in every cycle. When comparing the energy consump-

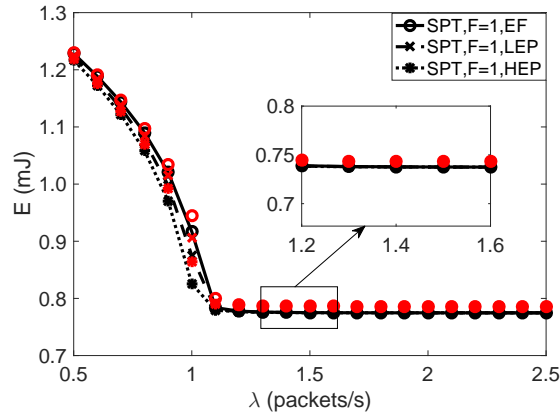


Figure 7: Energy consumption of SPT ($F = 1$) for different packet arrival rates.

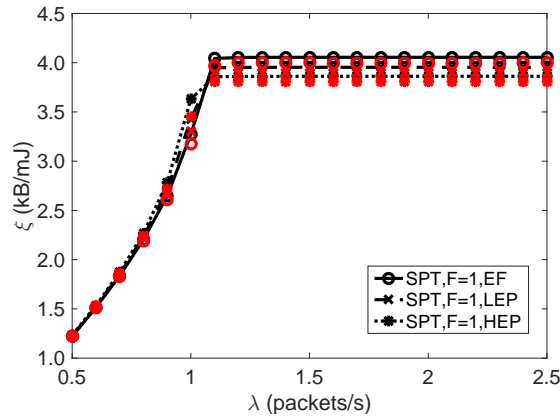


Figure 8: Energy efficiency of SPT ($F = 1$) for different packet arrival rates.

485 tion under various channel conditions in the zoomed-in subfigure in Figure 7,
we notice that the energy consumption difference is almost negligible. This is
because the occurrence of erroneous frames increases retransmissions and keeps
the packets in the queues of the nodes for a longer time, exacerbating the con-
gestion status of already congested nodes. This effect reinforces the effect that
490 nodes remain active in all cycles.

Figure 8 displays the variation of the energy efficiency with a traffic load
under different channel conditions. The same as observed above, two operating
regions exist, i.e., the unsaturated and the saturated. With a higher traffic

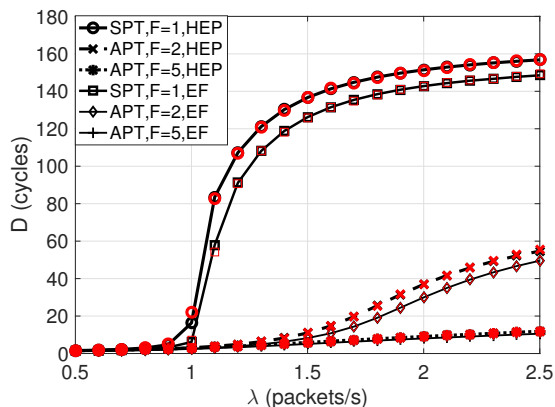


Figure 9: Delay for different packet arrival rates.

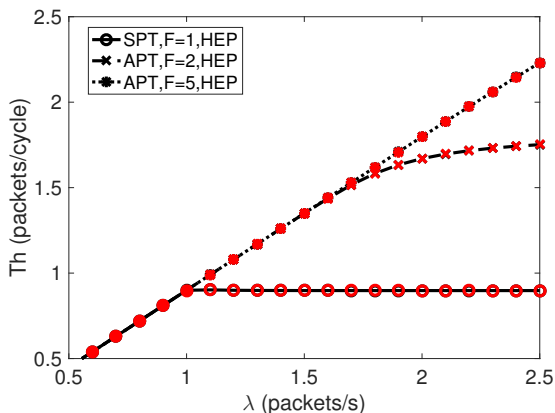


Figure 10: Throughput for different packet arrival rates.

load before saturation, the throughput increases and the energy consumption
 495 decreases, leading to a rapid growth in energy efficiency. In the saturated region,
 however, the difference in energy efficiency for different channel conditions is
 small. As expected, the poorer the channel condition the worse the energy
 efficiency.

7.3. Performance of APT versus SPT in CPTS Mode

500 Figure 9 illustrates the delay performance as traffic load varies under the
 EF and HEP channel conditions for different frame lengths (F). As observed,
 the impact that channel condition has on delay performance is less significant

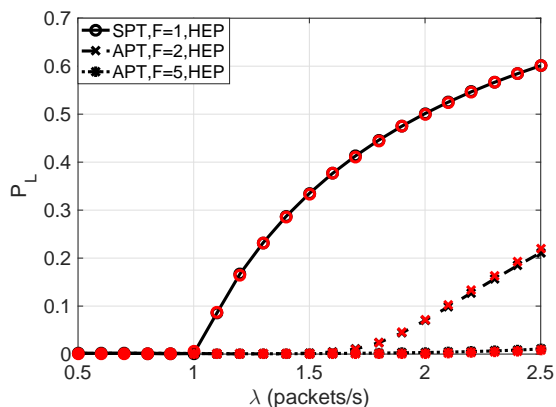


Figure 11: Packet loss for different packet arrival rates.

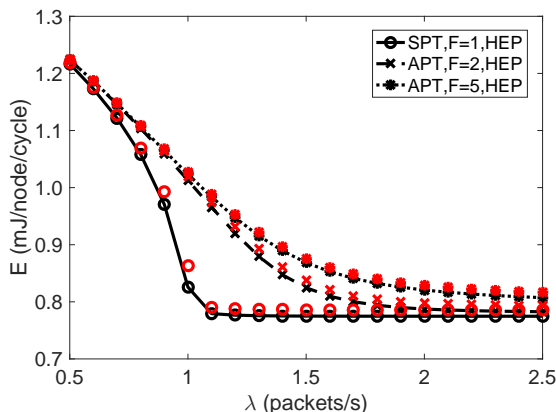


Figure 12: Energy consumption for different packet arrival rates.

with a larger F , even under severe channel impairment (HEP). This result is caused by the fact that the larger the F , the higher the fraction of time the queues of the nodes remain empty. This fact leads to a smaller number of active nodes contending per cycle on average, and therefore, to shorter retransmission times to recover from both collisions and failed frames delivery due to channel impairments. This observation coincides with the fact that a higher traffic load is required to reach the saturation point with a larger F .

The evolution of the total network throughput and the packet loss with traffic load for different frame lengths (F) under the HEP channel condition is depicted in Figures 10 and 11, respectively. Note that in these figures, the

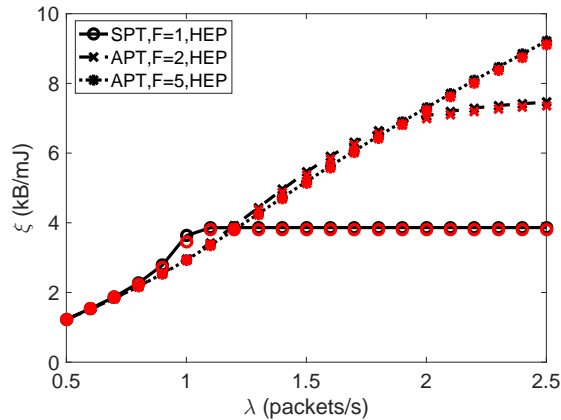


Figure 13: Energy efficiency for different packet arrival rates.

values are approximately 5% lower than the ones obtained with the EF channel condition.

515 Figures 12 and 13 display respectively the variation of the average energy consumption per node and cycle, and the average node energy efficiency, with traffic load under the HEP channel condition. Observe in Figure 12 that the energy consumption increases with a larger F . This can be explained by the same reason as described previously, i.e., the larger the F the higher the frac-
 520 tion of cycles with all nodes inactive. In such cycles, energy is wasted due to idle listening when operating in the CPTS energy mode. However, the energy efficiency increases with a larger F , as shown in Figure 13.

An interesting observation that helps to illustrate the previously described effect is shown in Figure 13 at loads around $\lambda = 1$ packet/s. At these loads, the
 525 energy efficiency operating with $F = 1$ is higher than that of when operating with $F = 2$. The energy efficiency depends directly on the node throughput and it is inversely proportional to the energy consumption, as shown in (32). When operating with $F = 1$ around the observed load ($\lambda = 1$), the energy consumption is the dominant factor, as increasing the load makes the energy consumption
 530 decrease faster for $F = 1$ than for $F = 2$. In addition, the throughput difference for loads slightly below $\lambda = 1$ packet/s is negligible for both values of F . However, as the load increases above $\lambda = 1$, the throughput becomes the domi-

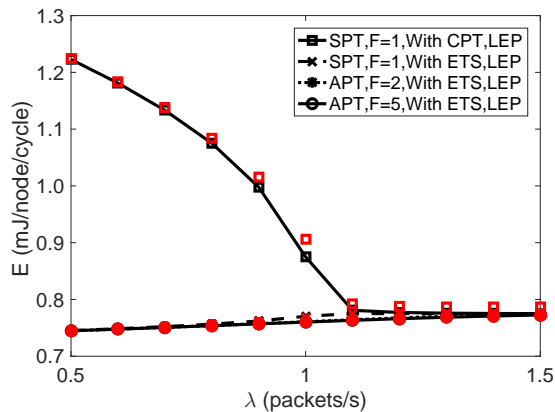


Figure 14: Energy consumed by the RN per cycle with and without ETS.

nant factor. Note that the achieved throughput stabilizes when operating with $F = 1$. So does the energy consumption. When operating with $F = 2$, however, the throughput keeps on increasing and, in addition, the energy consumption keeps on decreasing.

Table 2: Total Energy Consumption (mJ) for 100 Cycles

Mode	SPT, $F = 1$	APT, $F = 2$	APT, $F = 5$
CPTS (EF ch.)	74.774	74.087	74.893
CPTS (LEP ch.)	69.719	75.118	75.184
ETS (EF ch.)	54.445	54.759	54.114
ETS (LEP ch.)	55.195	54.889	54.781

7.4. Performance of the ETS Energy Mode

Figure 14 shows the average energy consumed by a node per cycle as a function of the load when deploying the CPTS and ETS energy modes. Observe that the ETS mode saves, on average, over 60% energy consumption in comparison with the CPTS mode, when the network operates in SPT and with very low load. For SPT, however, the energy consumptions of both the CPTS and ETS energy modes coincide when the network is saturated. This behavior highlights the fact that the energy saved by the ETS mode is particularly significant in low loads, when almost all nodes are inactive in the majority of the cycles. Further-

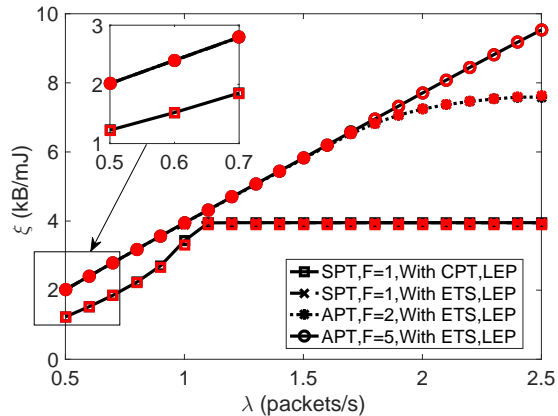


Figure 15: Energy efficiency of the RN with and without ETS.

more, it is worth mentioning that when deploying the ETS mode, the energy consumption is almost insensitive to the value of the maximum frame length F .

For illustration purpose, Table 2 compares the total average energy consumed during 100 consecutive cycles with different combinations of the proposed energy modes, channel conditions, and different values of F , when $\lambda = 0.5$ packets/s. Note that these values are obtained from simulations, and they do not need to correspond to those obtained for 100 standard cycles in the stationary regime. As observed, the energy consumed in the ETS energy mode is approximately 36% lower than with the CPTS mode under the EF channel condition, and approximately 26% lower than under the LEP channel condition. As mentioned before, the energy consumption is almost insensitive to the value of F in the ETS energy mode. Moreover, for $F = 1$, the energy consumption in the CPTS energy mode under LEP channel condition is lower than under the EF channel condition. This can be again explained by the fact that in the CPTS energy mode the energy is mainly wasted due to idle listening in cycles with no active nodes, which occurs less frequently as the channel condition deteriorates. As mentioned before, as F increases, the energy consumption in the CPTS energy mode is less dependent on F .

Figure 15 plots the variation of the energy efficiency expressed as kB/mJ for different loads, energy modes and under the LEP channel condition. It is evident

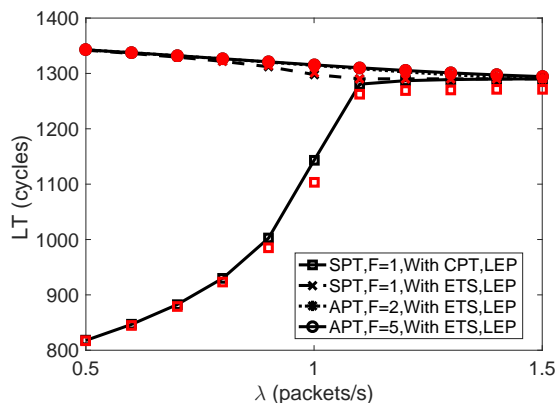


Figure 16: Lifetime of the RN with and without ETS.

that for SPT and low loads, the energy efficiency of the ETS energy mode is higher than the efficiency of the CPTS energy mode. By looking at the zoomed-in subfigure in Figure 15, we find that the energy efficiency improvement can be larger than 70% at low loads. However, as the load increases they converge
570 to the same value, particularly once saturation is achieved.

The lifetime of a node, i.e., the number of consecutive cycles the node can operate with an initial energy $E_{initial} = 1$ J under the LEP channel condition is shown in Figure 16, as a function of the load and energy modes. Again, it is clear that for low loads the lifetime improvement when deploying the ETS
575 energy mode with respect to the CPTS mode is longer than 65%. However, as the load increases the lifetimes with both energy modes tend to the same value.

8. Conclusions

In this paper, we developed a 4D DTMC to model the behavior of synchronous duty-cycled MAC protocols for WSNs with error-prone wireless channels. One of the dimensions in the network state vector describes the evolution
580 of the channel condition over time. In the proposed model, the channel condition can be classified in two different macro-states. In one of them, frames are received with no channel error, provided that they do not collide. In the other one, frames that do not collide can be received with channel error, and the error

585 probability is an increasing function of the frame length, which makes it more realistic.

Closed-form expressions are derived for the average packet queuing delay, packet loss probability, node and network throughput, average energy consumption per node, and energy efficiency. The numerical results obtained by the analytical model match closely those obtained through simulations, confirming
590 the accuracy of the analytical model. These results also reveal the impact that transmission errors have on network performance, as well as the benefits brought by the APT scheme in both error-free and error-prone environments.

Finally, it is demonstrated that the proposed ETS energy mode can substantially extend the lifetime of the network, **particularly by 70%in light traffic application scenarios.**
595

References

- [1] M. R. Palattella, M. Dohler, Al. Grieco, G. Rizzo, J. Torsner, T. Engel, L. Ladid, Internet of things in the 5G era: Enablers, architecture, and business
600 models, *IEEE J. Sel. Areas Commun.* 34 (3) (2016) 510-527.
- [2] A. Boukerche, X. Zhou, MAC transmission protocols for delay-tolerant sensor networks, *Computer Networks* 124 (2017) 108-125.
- [3] L. Guntupalli, J. Martinez-Bauset, F. Y. Li, M. A. Weitnauer, Aggregated packet transmission in duty-cycled WSNs: Modeling and performance evaluation,
605 *IEEE Trans. Veh. Technol.* 66 (1) (2017) 563-579.
- [4] S. Saginbekov, A. Jhumka, Many-to-many data aggregation scheduling in wireless sensor networks with two sinks, *Computer Networks* 123 (2017) 184-199.
- [5] B. Holfeld, D. Wieruch, T. Wirth, L. Thiele, S. A. Ashraf, J. Huschke,
610 I. Aktas, J. Ansari, Wireless communication for factory automation: an opportunity for LTE and 5G systems, *IEEE Commun. Mag.* 54 (6) (2016) 36-43.

- [6] S. Kurt, H. U. Yildiz, M. Yigit, B. Tavli, V. C. Gungor, Packet size optimization in wireless sensor networks for smart grid applications, *IEEE Trans. Indus. Elect.* 64 (3) (2017) 2392-2401. 615
- [7] Y. Sankarasubramaniam, I. F. Akyildiz, S. W. Mclaughlin, Energy efficiency based packet size optimization in wireless sensor networks, in: *Proc. IEEE Int. Workshop Sensor Netw. Protocols Appl. (SNPA)*, 2003, pp. 1-8.
- [8] L. Guntupalli, F. Y. Li, J. Martinez-Bauset, Event-triggered sleeping for synchronous DC MAC in WSNs: Mechanism and DTMC modeling, in: *Proc. IEEE GLOBECOM*, 2016, pp. 1-6. 620
- [9] W. Ye, J. Heidemann, D. Estrin, Medium access control with coordinated adaptive sleeping for wireless sensor networks, *IEEE/ACM Trans. Netw.* 12 (3) (2004) 493-506.
- [10] J. Martinez-Bauset, L. Guntupalli, F. Y. Li, Performance analysis of synchronous duty-cycled MAC protocols, *IEEE Wireless Commun. Lett.* 4 (5) (2015) 469-472. 625
- [11] O. Yang, W. Heinzelman, Modeling and performance analysis for duty-cycled MAC protocols in wireless sensor networks, *IEEE Trans. Mobile Comput.* 11 (6) (2012) 905-921. 630
- [12] O. Yang, W. Heinzelman, Modeling and throughput analysis for S-MAC with a finite queue capacity, in: *Proc. IEEE ISSNIP*, 2009, pp. 409414.
- [13] F. Tong, L. Zheng, M. Ahmadi, M. Li, J. Pan, Modeling and analyzing duty-cycling, pipelined-scheduling MACs for linear sensor networks, *IEEE Trans. Veh. Technol.* 65 (4) (2016) 2608-2620. 635
- [14] L. Guntupalli, J. Martinez-Bauset, F. Y. Li, Cooperative or non-cooperative transmission in synchronous DC WSNs: A DTMC-based approach, in: *Proc. IEEE ICC*, 2017, pp. 1-6.

- [15] X. Zhou, A. Boukerche, AFLS: An adaptive frame length aggregation
640 scheme in vehicular networks, *IEEE Trans. Veh. Technol.* 66 (1) (2017)
855-867.
- [16] K. S. Deepak, A. V. Babu, Enhancing Reliability of IEEE 802.15.6 Wireless
Body Area Networks in Scheduled Access Mode and Error Prone Channels,
Wireless Personal Commun. 89 (2016) 93118.
- [17] X. Wang, J. Yin, D. Agrawal, Effects of contention window and packet
645 size on the energy efficiency of wireless local area network, in: *Proc. IEEE
WCNC, 2005*, pp. 16.
- [18] Y. Zhang and F. Shu, Packet size optimization for goodput and energy
efficiency enhancement in slotted IEEE 802.15.4 networks, in: *Proc. IEEE
650 WCNC, 2009*, pp. 16.
- [19] M. Krishnan, E. Haghani, and A. Zakhori, Packet length adaptation in
WLANs with hidden nodes and time-varying channels, in: *Proc. IEEE
GLOBECOM, 2011*, pp. 16.
- [20] W. Dong, J. Yu, P. Zhang, Exploiting error estimating codes for packet
655 length adaptation in low-power wireless networks, *IEEE Trans. Mobile
Comput.* 14 (8) (2015) 1601-1614.
- [21] M. C. Vuran, I. F. Akyildiz, Cross-layer packet size optimization for wireless
terrestrial, underwater, and underground sensor networks, in: *Proc. IEEE
INFOCOM, 2008*, pp.226-230.
- [22] Y. Li, G. Ozcan, M. C. Gursoy, S. Velipasalar, Energy efficiency of hybrid-
660 ARQ under statistical queuing constraints, *IEEE Trans. Commun.* 64 (10)
(2016) 4253-4267.
- [23] R. Sassioui, M. Jabi, L. Szczecinski, L. B. Le, M. Benjillali, B. Pelletier,
HARQ and AMC: Friends or foes?, *IEEE Trans. Commun.* 65 (2) (2017)
665 635-650.

- [24] A. Akbas , H. U. Yildiz, B. Tavli, S. Uludag, Joint optimization of transmission power level and packet size for WSN lifetime maximization, *IEEE Sensors Journal* 16 (12) (2016) 5084-94.
- [25] G. Bartoli, N. Beaulieu, R. Fantacci, D. Marabissi, An effective multiuser
670 detection scheme for MPR random access networks, *IEEE Trans. Comm.* 65 (3) (2017) 1119-1130.
- [26] Y. Wu, G. Zhou, J. A. Stankovic, ACR: Active collision recovery in dense wireless sensor networks, in: *Proc. IEEE INFOCOM*, 2010, pp. 1-9.
- [27] O. M. Abu-Sharkh, A. H. Tewfik, Toward accurate modeling of the IEEE
675 802.11e EDCA under finite load and error-prone channel, *IEEE Trans. Wireless Commun.* 7 (7) (2008) 2560-2570.
- [28] P. Ji, B. Liu, D. Towsley, Z. Ge, J. Kurose, Modeling frame-level errors in GSM wireless channels, *Performance Evaluation* 55 (1) (2004) 165-181.
- [29] G. Boggia, P. Camarda, A. D'Alconzo, Performance of Markov models for
680 frame-level errors in IEEE 802.11 wireless LANs, *Int. J. Commun. Syst.*, 22 (6) (2009) 695-718.
- [30] D. Striccoli, G. Boggia, A. Grieco, A Markov model for characterizing IEEE 802.15. 4 MAC layer in noisy environments, *IEEE Trans. Ind. Electron.* 62 (8) (2015) 5133-5142.
- [31] S. Robert, J.-Y. Le Boudec, New models for pseudo self-similar traffic,
685 *Performance Evaluation* 30 (1) (1997) 57-68.

Appendix

Table .3: Transition Probabilities for P_{EP}

Notation used for important parameters in this table and throughout the paper.	
T : Duration of a cycle; W : Contention window size	K : Maximum number of active nodes in the network,
λ : DATA packet arrival rate at each node	other than the RN, $K = N - 1$,
$A_{\geq i}$: Probability of i or more packets arriving in a cycle;	A_i : Probability of i packets arriving in a cycle; $A_i = e^{-\lambda T} (\lambda T)^i / i!$,
$\hat{A} = 1 - A_0$,	$B_k(K)$: Probability that k nodes, out of K that have
\hat{T}_k : Probability that the RN does not transmit when	their queues empty, receive packets in a cycle; $B_k(K) = \binom{K}{k} \hat{A}^k A_0^{K-k}$,
contending with other k nodes and two or more of the	S_k : Probability that an active node transmits a frame successfully in
other nodes collide; $1 - (k+1)P_{s,k} - P_{f,k}$,	a cycle where k nodes contend, $S_k = kP_{s,k-1}$, $\hat{S}_k : 1 - S_k$,
α : Number of packets aggregated for transmission.	P_e : Probability that the queue of an active node becomes empty conditioned
When node is in state i , $\alpha = \min(i, F)$,	on a successful transmission; $P_e = P_s A_0 \sum_{i=1}^F \pi_i / P_s (1 - \pi_0)$, $\hat{P}_e : 1 - P_e$.
No active node exists. Transitions occur due to new arrivals	
$P_{(0,0,0),(j,l,0)} = B_l(K) \cdot A_j$; $0 \leq j < Q$, $0 \leq l \leq K$,	$P_{(0,0,0),(Q,l,0)} = B_l(K) \cdot A_{\geq Q}$; $0 \leq l \leq K$.
No packets in the queue of the RN, i.e., no transmissions by the RN. Transitions are caused by the other k active nodes	
$P_{(0,k,0),(j,l,0)} = S^e \cdot S_k \cdot P_e \cdot B_{l-k+1}(K-k) \cdot A_j$ $+ S^e \cdot S_k \cdot \hat{P}_e \cdot B_{l-k}(K-k) \cdot A_j$ $+ \left[(1 - S^e) S_k + \hat{S}_k \right] \cdot B_{l-k}(K-k) \cdot A_j$; $0 \leq j < Q$, $1 \leq k \leq l < K$,	$P_{(0,k,0),(Q,l,0)} = S^e \cdot S_k \cdot P_e \cdot B_{l-k+1}(K-k) \cdot A_{\geq Q}$ $+ S^e \cdot S_k \cdot \hat{P}_e \cdot B_{l-k}(K-k) \cdot A_{\geq Q}$ $+ \left[(1 - S^e) S_k + \hat{S}_k \right] \cdot B_{l-k}(K-k) \cdot A_{\geq Q}$; $1 \leq k \leq l < K$,
$P_{(0,k,0),(j,K,0)} = S^e \cdot S_k \cdot \hat{P}_e \cdot B_{K-k}(K-k) \cdot A_j$ $+ \left[(1 - S^e) S_k + \hat{S}_k \right] \cdot B_{K-k}(K-k) \cdot A_j$; $0 \leq j < Q$, $1 \leq k \leq K$,	$P_{(0,k,0),(Q,K,0)} = S^e \cdot S_k \cdot \hat{P}_e \cdot B_{K-k}(K-k) \cdot A_{\geq Q}$ $+ \left[(1 - S^e) S_k + \hat{S}_k \right] \cdot B_{K-k}(K-k) \cdot A_{\geq Q}$; $1 \leq k \leq K$,
$P_{(0,k,0),(j,k-1,0)} = S^e \cdot S_k \cdot P_e \cdot B_0(K-k) \cdot A_j$; $0 \leq j < Q$, $1 \leq k \leq K$,	$P_{(0,k,0),(Q,k-1,0)} = S^e \cdot S_k \cdot P_e \cdot B_0(K-k) \cdot A_{\geq Q}$; $1 \leq k \leq K$.
$k+1$ nodes including the RN are active. Successful transmission by the RN in its first attempt or by any other node	
$P_{(i,k,0),(j,l,0)} = S_\alpha^e \cdot P_{s,k} \cdot B_{l-k}(K-k) \cdot A_j$; $1 \leq i \leq F$, $0 \leq j \leq i-1$, $0 \leq k \leq l \leq K$,	$P_{(i,k,0),(j,l,0)} = S_\alpha^e \cdot P_{s,k} \cdot B_{l-k}(K-k) \cdot A_{j-i+F}$; $F+1 \leq i \leq Q$, $i-F \leq j \leq i-1$, $0 \leq k \leq l \leq K$,
$P_{(i,k,0),(j,l,0)} = S_\alpha^e \cdot P_{s,k} \cdot B_{l-k}(K-k) \cdot A_{j-i+\alpha}$ $+ S^e \cdot k P_{s,k} \cdot P_e \cdot B_{l-k+1}(K-k) \cdot A_{j-i}$ $+ S^e \cdot k P_{s,k} \cdot \hat{P}_e \cdot B_{l-k}(K-k) \cdot A_{j-i}$ $+ (1 - S^e) \cdot k P_{s,k} \cdot B_{l-k}(K-k) \cdot A_{j-i}$ $+ \hat{T}_k \cdot B_{l-k}(K-k) \cdot A_{j-i}$; $1 \leq i \leq j < Q$, $1 \leq k \leq l < K$,	$P_{(i,k,0),(Q,l,0)} = S_\alpha^e \cdot P_{s,k} \cdot B_{l-k}(K-k) \cdot A_{\geq Q-i+\alpha}$ $+ S^e \cdot k P_{s,k} \cdot P_e \cdot B_{l-k+1}(K-k) \cdot A_{\geq Q-i}$ $+ S^e \cdot k P_{s,k} \cdot \hat{P}_e \cdot B_{l-k}(K-k) \cdot A_{\geq Q-i}$ $+ (1 - S^e) \cdot k P_{s,k} \cdot B_{l-k}(K-k) \cdot A_{\geq Q-i}$ $+ \hat{T}_k \cdot B_{l-k}(K-k) \cdot A_{\geq Q-i}$; $1 \leq i \leq Q$, $1 \leq k \leq l < K$,
$P_{(i,k,0),(j,K,0)} = S_\alpha^e \cdot P_{s,k} \cdot B_{K-k}(K-k) \cdot A_{j-i+\alpha}$ $+ S^e \cdot k P_{s,k} \cdot \hat{P}_e \cdot B_{K-k}(K-k) \cdot A_{j-i}$ $+ (1 - S^e) \cdot k P_{s,k} \cdot B_{K-k}(K-k) \cdot A_{j-i}$ $+ \hat{T}_k \cdot B_{l-k}(K-k) \cdot A_{j-i}$; $1 \leq i \leq j < Q$, $1 \leq k \leq K$,	$P_{(i,k,0),(Q,K,0)} = S_\alpha^e \cdot P_{s,k} \cdot B_{K-k}(K-k) \cdot A_{\geq Q-i+\alpha}$ $+ S^e \cdot k P_{s,k} \cdot \hat{P}_e \cdot B_{K-k}(K-k) \cdot A_{\geq Q-i}$ $+ (1 - S^e) \cdot k P_{s,k} \cdot B_{K-k}(K-k) \cdot A_{\geq Q-i}$ $+ \hat{T}_k \cdot B_{l-k}(K-k) \cdot A_{\geq Q-i}$; $1 \leq i \leq Q$, $1 \leq k \leq K$.
$k+1$ nodes including the RN are active. Successful transmission by the RN after r failed attempts	
$P_{(i,k,r),(j,l,0)} = S_\alpha^e \cdot P_{s,k} \cdot B_{l-k}(K-k) \cdot A_j$; $1 \leq i \leq F$, $0 \leq j \leq i-1$, $0 \leq k \leq l < K$, $0 \leq r < R$,	$P_{(i,k,r),(j,l,0)} = S_\alpha^e \cdot P_{s,k} \cdot B_{l-k}(K-k) \cdot A_{j-i+F}$; $F+1 \leq i \leq Q$, $i-F \leq j \leq i-1$, $0 \leq k \leq l \leq K$, $0 \leq r < R$,
$P_{(i,k,r),(j,l,0)} = S_\alpha^e \cdot P_{s,k} \cdot B_{l-k}(K-k) \cdot A_{j-i+\alpha}$; $1 \leq i \leq j < Q$, $0 \leq k \leq l \leq K$, $0 \leq r \leq R$,	$P_{(i,k,r),(Q,l,0)} = S_\alpha^e \cdot P_{s,k} \cdot B_{l-k}(K-k) \cdot A_{\geq Q-i+\alpha}$; $1 \leq i \leq Q$, $0 \leq k \leq l \leq K$, $0 \leq r \leq R$,
$k+1$ nodes including the RN are active. Failed transmission by the RN	
$P_{(i,k,r),(j,l,r+1)} = P_{f,k} \cdot B_{l-k}(K-k) \cdot A_{j-i}$; $+ (1 - S_\alpha^e) \cdot P_{s,k} \cdot B_{l-k}(K-k) \cdot A_{j-i}$; $1 \leq i \leq j < Q$, $0 \leq k \leq l \leq K$, $0 \leq r < R$,	$P_{(i,k,r),(Q,l,r+1)} = P_{f,k} \cdot B_{l-k}(K-k) \cdot A_{\geq Q-i}$; $+ (1 - S_\alpha^e) \cdot P_{s,k} \cdot B_{l-k}(K-k) \cdot A_{\geq Q-i}$; $1 \leq i \leq Q$, $0 \leq k \leq l \leq K$, $0 \leq r < R$.
$P_{(i,k,R),(j,l,0)} = P_{sf,k} \cdot B_{l-k}(K-k) \cdot A_{j-i+\alpha}$; $1 \leq i \leq Q$, $i-\alpha \leq j < Q$, $0 \leq k \leq l \leq K$,	$P_{(i,k,R),(Q,l,0)} = P_{sf,k} \cdot B_{l-k}(K-k) \cdot A_{\geq Q-i+\alpha}$; $1 \leq i \leq Q$, $0 \leq k \leq l \leq K$.
$k+1$ nodes including the RN are active. The RN loses access contention	
$P_{(i,k,r),(j,l,r)} = S^e \cdot k P_{s,k} \cdot P_e \cdot B_{l-k+1}(K-k) \cdot A_{j-i}$ $+ S^e \cdot k P_{s,k} \cdot \hat{P}_e \cdot B_{l-k}(K-k) \cdot A_{j-i}$ $+ (1 - S^e) \cdot k P_{s,k} \cdot B_{l-k}(K-k) \cdot A_{j-i}$ $+ \hat{T}_k \cdot B_{l-k}(K-k) \cdot A_{j-i}$; $1 \leq i \leq j < Q$, $1 \leq k \leq l < K$, $0 \leq r \leq R$,	$P_{(i,k,r),(Q,l,r)} = S^e \cdot k P_{s,k} \cdot P_e \cdot B_{l-k+1}(K-k) \cdot A_{\geq Q-i}$ $+ S^e \cdot k P_{s,k} \cdot \hat{P}_e \cdot B_{l-k}(K-k) \cdot A_{\geq Q-i}$ $+ (1 - S^e) \cdot k P_{s,k} \cdot B_{l-k}(K-k) \cdot A_{\geq Q-i}$ $+ \hat{T}_k \cdot B_{l-k}(K-k) \cdot A_{\geq Q-i}$; $1 \leq i \leq Q$, $1 \leq k \leq l < K$, $0 \leq r \leq R$,
$P_{(i,K,r),(j,K,r)} = S^e \cdot K P_{s,K} \cdot \hat{P}_e \cdot A_{j-i}$ $+ (1 - S^e) \cdot K P_{s,K} \cdot A_{j-i} + \hat{T}_K \cdot A_{j-i}$; $1 \leq i \leq j < Q$, $0 \leq r \leq R$,	$P_{(i,K,r),(Q,K,r)} = S^e \cdot K P_{s,K} \cdot \hat{P}_e \cdot A_{\geq Q-i}$ $+ (1 - S^e) \cdot K P_{s,K} \cdot A_{\geq Q-i} + \hat{T}_K \cdot A_{\geq Q-i}$; $1 \leq i \leq Q$, $0 \leq r \leq R$,
$P_{(i,k,r),(j,k-1,r)} = S^e \cdot k P_{s,k} \cdot P_e \cdot B_0(K-k) \cdot A_{j-i}$; $1 \leq i \leq j < Q$, $1 \leq k \leq K$, $0 \leq r \leq R$,	$P_{(i,k,r),(Q,k-1,r)} = S^e \cdot k P_{s,k} \cdot P_e \cdot B_0(K-k) \cdot A_{\geq Q-i}$; $1 \leq i \leq Q$, $1 \leq k \leq K$, $0 \leq r \leq R$.